Splitting of an electromagnetically induced transparency window of rubidium atoms in a static magnetic field

Xiao-Gang Wei,[1,2] Jin-Hui Wu,[1,2] Gui-Xia Sun,[1,2] Zhuang Shao,[1,2] Zhi-Hui Kang,[1,2] Yun Jiang,[1,2] and Jin-Yue Gao[1,2,3,*]
[1]*College of Physics, Jilin University, Changchun 130023, China*
[2]*Key Laboratory of Coherent Light and Atomic and Molecular Spectroscopy of Ministry of Education, Jilin University, China*
[3]*CCAST (World Laboratory), P. O. Box 8370, Beijing 100080, China*
(Received 25 March 2005; published 8 August 2005)

We study the phenomenon of electromagnetically induced transparency (EIT) of ^{87}Rb vapor at the temperature of 325 K in a magnetic field. Two linearly polarized orthogonal laser fields act on two dipole-allowed transitions of the $D1$ line of ^{87}Rb in the Λ configuration, respectively. In the absence of magnetic fields, we observe a wide EIT window with the contrast of about 66% while when the magnetic field is applied, the wide EIT window is split into three or four narrower subwindows with contrasts of 32% or 16% due to the lifting of magnetic sublevels' degeneracy. The number of EIT subwindows depends on the magnetic field orientation. Our theoretical simulations and analysis are in good agreement with the experimental results.

DOI: 10.1103/PhysRevA.72.023806 PACS number(s): 42.50.Gy, 42.50.Hz

I. INTRODUCTION

Electromagnetically induced transparency (EIT) is based on coherent population trapping (CPT) [1] and refers to a phenomenon that, in an absorbing medium driven by a coupling field, a probe field will experience reduced absorption at the center of the probe transition. Since the phenomenon of EIT was first proposed [2] and observed [3], it has attracted great attention along with its applications and the related effects such as lasing without population inversion (LWI) [4], enhancement of nonlinear optical effects [5], and enchantment of the refractive index without absorption [6]. Up to now, a lot of theoretical and experimental works on EIT using atomic vapors [7] or solid state materials [8] as the interaction media have been successfully carried out. However, most investigations are based on simplified three-level models, while actual systems generally involve more complicated situations due to the magnetic structure of the concerned levels. So, the EIT phenomenon and its related effects in coherently prepared media have to be studied more carefully.

Recently, it has been shown that magnetic fields could play important roles in such phenomena based on quantum interference and atomic coherence [9]. For instance, one can observe sub-natural-width positive or negative resonance in degenerate two-level atomic systems by inducing coherence among magnetic sublevels, which are frequency shifted by a magnetic field [10]. It is more important that this phenomenon could lead to a novel all-optical magnetometer with sensitivity potentially surpassing the state-of-the-art devices [11]. However, to our knowledge, no theoretical or experimental works on EIT in Doppler-broadened three-level atomic vapors with a magnetic field lifting the degeneracy of involved hyperfine levels have been reported.

In this paper, we investigate the EIT phenomenon of atomic ^{87}Rb at the temperature of 325 K with a static magnetic field lifting the degeneracy of all three involved hyperfine levels. Two collinearly propagating and linearly polarized laser fields (a probe field and a coupling field) are used to couple one hyperfine level (the upper level) of the $5P_{1/2}$ state to two hyperfine levels (the lower levels) of the $5S_{1/2}$ state, respectively. In the case of zero magnetic fields, we observed a deep EIT window with the contrast of about 66%. Here, the EIT window width is limited by both the spontaneous decay rate of the upper level and the coupling field intensity. When a magnetic field parallel to both laser beams is applied, the EIT window is split into three narrower subwindows with contrasts of about 32%. If the magnetic field is perpendicular to the laser beams, however, the EIT window is split into four narrower subwindows whose contrasts are 32% or 16%. This is because the decomposition of the linearly polarized optical fields strongly depends on the orientation of the used magnetic field. By simple theoretical analyses and simulations, we also show how an ideal degenerate three-level atomic system is split into several three-level subsystems by a magnetic field. Our theoretical calculations are in good agreement with the experimental results.

II. THEORETICAL MODELS AND EQUATIONS

We show the relevant hyperfine levels of ^{87}Rb atoms in Fig. 1(a), where the hyperfine level $F'=2$ of $5P_{1/2}$ state serves as the excited level $|3\rangle$, and hyperfine levels $F=1$ and $F=2$ of $5S_{1/2}$ state serve as the ground levels $|1\rangle$ and $|2\rangle$, respectively. Levels $|2\rangle$ and $|3\rangle$ are coupled by an intense laser with frequency ω_c (the coupling field). A weak laser with frequency ω_p (the probe field) is used to detect the absorption between levels $|2\rangle$ and $|3\rangle$. In the absence of magnetic fields, the coherently driven ^{87}Rb atom can be regarded as an ideal three-level Λ system, while when a magnetic field is used, the degeneracy of all three involved hyperfine levels will be broken so that the ^{87}Rb atom has to be treated as a complicated system with 13 nondegenerate magnetic sublevels. The energy splitting for any two adjacent magnetic sublevels of a hyperfine level is

*Corresponding author. Email address: jygao@mail.jlu.edu.cn

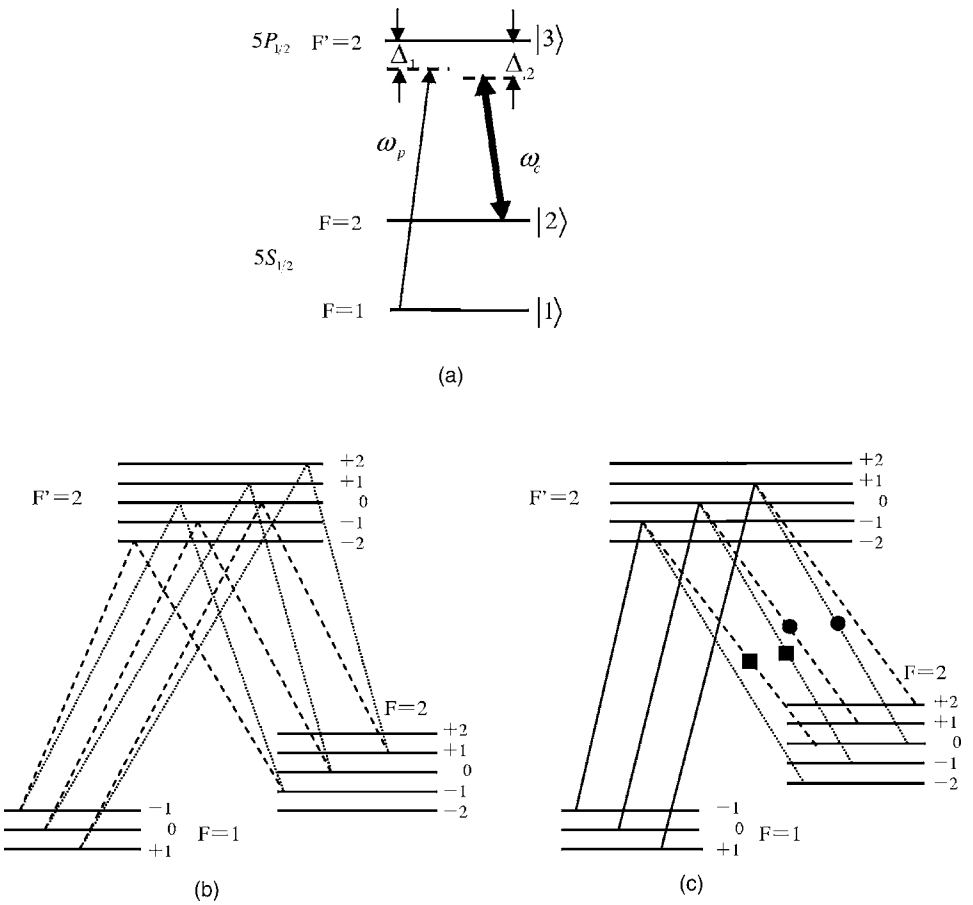

FIG. 1. (a) Energy diagram of atomic ^{87}Rb driven by two linearly polarized coherent lasers (a probe field and a coupling field) in the absence of magnetic fields. (b) Energy diagram of atomic ^{87}Rb when the magnetic field is parallel to the laser propagation direction where both fields should be seen as circularly polarized. (c) Energy diagram of atomic ^{87}Rb when the magnetic field is orthogonal to the laser propagation direction where the coupling field should be seen as circularly polarized, while the probe field is still seen as linearly polarized. The two subsystems denoted by solid squares (circles) are degenerate.

$$\Delta = \frac{g_F \mu_B B}{\eta} \tag{1}$$

with $g_F = g_J[F(F+1)+J(J+1)-I(I+1)]/[2F(F+1)]$ being the composite Lande factor and μ_B being the Bohr magneton. In the limit of a weak probe, we just have to consider one- and two-photon processes, while all other multiple-photon processes can be ignored. In this case, the coherently driven ^{87}Rb atom can be regarded as the superposition of several independent three-level subsystems. It should be borne in mind, however, the way by which the independent three-level subsystems superpose strongly depending on the magnetic field orientation.

For the ideal three-level system as shown in Fig. 1(a), with the electricdipole approximation and the rotating-wave approximation, in the limit of a weak probe, we can first obtain the density matrix equations, and then get the steady-state solution for the nondiagonal element ρ_{31} as

$$\rho_{31}^{a} = -\frac{i\Omega_p}{\frac{\gamma}{2} + i\Delta_1 + \frac{\Omega_c^2}{\Gamma_3 + i(\Delta_1 - \Delta_2)}}, \tag{2}$$

where $\gamma = \Gamma_1 + \Gamma_2 + \Gamma_3$, Γ_1 and Γ_2, respectively being the spontaneous decay rates from level $|3\rangle$ to levels $|1\rangle$ and $|2\rangle$, and Γ_3 representing the nonradiative decay rate between levels $|1\rangle$ and $|2\rangle$. $\Delta_1 = \omega_{31} - \omega_p$ and $\Delta_2 = \omega_{32} - \omega_c$ are detunings of the probe and coupling fields, respectively. $\Omega_p = \vec{E}_p \cdot \vec{\mu}_{31}/2\eta$ and $\Omega_c = \vec{E}_c \cdot \vec{\mu}_{32}/2\eta$ are Rabi frequencies of the probe and coupling fields, respectively.

In the case where the magnetic field is parallel to the laser propagation direction, polarizations of both probe and coupling fields are perpendicular to the magnetic field, so both laser fields should be viewed as composed of circularly polarized photons but not linearly polarized photons, which leads to the ideal three-level system split into six three-level subsystems as shown in Fig. 1(b). We set $\Delta_p = \omega_p - \omega_{0p}$ and $\Delta_c = \omega_c - \omega_{0c}$, where ω_{0p} corresponds to the resonant frequency of the probe transition $F=1, m_f=0 \leftrightarrow F'=2, m_f=0$, while ω_{0c} corresponds to the resonant frequency of the coupling transition $F=2, m_f=0 \leftrightarrow F'=2, m_f=0$. For the subsystem consisting of $F=1, m_f=-1$, $F=2, m_f=-1$, and $F'=2, m_f=-2$, if the probe field is at resonance, we have $\Delta_p = -3\Delta$, while if the coupling field is at resonance, we have $\Delta_c = -\Delta$. It is well known that, in order to observe the EIT window in a three-level Λ system, the two-photon resonance condition $\Delta_p - \Delta_c = -2\Delta$ should be satisfied. Thus, the EIT window should exist at $\Delta_p = -2\Delta$ if we set $\Delta_c = 0$. Similarly, for the subsystem consisting of $F=1, m_f=-1$, $F=2, m_f=-1$, and $F'=2, m_f=0$, the two-photon resonance condition is $\Delta_p - \Delta_c = -2\Delta$, and the EIT window should be at $\Delta_p = -2\Delta$ if we fix $\Delta_c = 0$. So, the two subsystems mentioned above are degenerate as long as EIT windows are concerned. With the same approach, we can see that EIT windows of the remaining four subsystems are respectively located at $\Delta_p = 0$ and $\Delta_p = 2\Delta$ if we fix $\Delta_c = 0$. That is, the six three-level subsystems can be treated as three sets of independent systems

(each set consists of two subsystems), which are distinguished from each other just by locations of their EIT windows. Thus, Eq. (2) should be rewritten as

$$\rho_{31}^{b} = -\frac{2i\Omega_p}{\frac{\gamma}{2} + i(\Delta_1 + 2\Delta) + \frac{(\Omega_c/\sqrt{2})^2}{\Gamma_3 + i(\Delta_1 + 2\Delta - \Delta_2)}} - \frac{2i\Omega_p}{\frac{\gamma}{2} + i\Delta_1 + \frac{(\Omega_c/\sqrt{2})^2}{\Gamma_3 + i(\Delta_1 - \Delta_2)}} - \frac{2i\Omega_p}{\frac{\gamma}{2} + i(\Delta_1 - 2\Delta) + \frac{(\Omega_c/\sqrt{2})^2}{\Gamma_3 + i(\Delta_1 - 2\Delta - \Delta_2)}}. \quad (3)$$

If the magnetic field is orthogonal to the laser propagation direction, only the coupling polarization is perpendicular to the magnetic field, so the coupling field should be viewed as composed of circularly polarized photons, while the probe field is still linearly polarized. In this case, the ideal three-level system is split into three four-level tripod subsystems as shown in Fig. 1(c). If the frequency difference between the lower levels in a tripod subsystem is relative large, the probe field must be far away from two-photon resonance with one coupling field when it is exactly on two-photon resonance with the other one. This is because the two circularly polarized coupling fields originate from the same laser and thus have the same frequencies. The two-photon off-resonance coupling field has little effect on the EIT subwindow contributed by the two-photon on-resonance coupling field, so a tripod subsystem can be seen as composed of two three-level subsystems, and the ideal three-level system can be viewed as composed of six three-level subsystems, which can be further divided into four sets of independent systems (two sets consist of one subsystem, while other two sets consist of two subsystems) by the same approach as used in the last paragraph. These four sets of independent systems also can be distinguished from each other by locations of their EIT windows. Then, we have

$$\rho_{31}^{c} = -\frac{2i\Omega_p}{\frac{\gamma}{2} + i(\Delta_1 + 3\Delta) + \frac{(\Omega_c/\sqrt{2})^2}{\Gamma_3 + i(\Delta_1 + 3\Delta - \Delta_2)}} - \frac{2i\Omega_p}{\frac{\gamma}{2} + i(\Delta_1 + \Delta) + \frac{(\Omega_c/\sqrt{2})^2}{\Gamma_3 + i(\Delta_1 + \Delta - \Delta_2)}} - \frac{2i\Omega_p}{\frac{\gamma}{2} + i(\Delta_1 - \Delta) + \frac{(\Omega_c/\sqrt{2})^2}{\Gamma_3 + i(\Delta_1 - \Delta - \Delta_2)}} - \frac{2i\Omega_p}{\frac{\gamma}{2} + i(\Delta_1 - 3\Delta) + \frac{(\Omega_c/\sqrt{2})^2}{\Gamma_3 + i(\Delta_1 - 3\Delta - \Delta_2)}}. \quad (4)$$

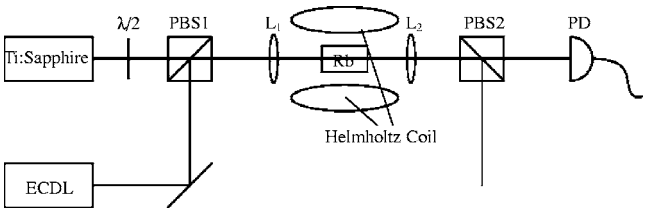

FIG. 2. Experimental setup for the investigation of EIT in hot ^{87}Rb atoms with a static magnetic field.

Noting that the absorption coefficient for the probe field is proportional to the imaginary part of the linear susceptibility, which is given by

$$\chi = \frac{N_0 \mu_{31}^2}{\varepsilon_0 \eta} \frac{\rho_{31}}{\Omega_p} \quad (5)$$

with N_0 being the atomic density, we can use Eqs. (2)–(4) to calculate the probe absorption in cases where the magnetic field is applied or not. Considering the Doppler broadening effect in hot ^{87}Rb atoms, we should use $N(v) = N_0 \exp(-v^2/v_p^2)/(v_p\sqrt{\pi})$ (where v_p is the most probable speed of atoms at given temperature), $\Delta_1 + \omega_p v/c$ and $\Delta_2 + \omega_c v/c$ to replace Δ_1, Δ_2 and N_0, and then integrate $\rho_{31}(v)$ for getting the total probe absorption.

III. EXPERIMENTAL SETUP

The experimental setup is shown in Fig. 2. The ^{87}Rb atomic vapor contained in a 3 cm long and 3 cm in diameter cylindrical cell is heated to the temperature of about 325 K. A Ti:sapphire ring laser (Coherent 899 ring laser system) with a line width of 500 kHz is tuned to the transition of $5S_{1/2}, F=1 \leftrightarrow 5P_{1/2}, F'=2$ acting as the probe field, which can scan over 20 GHz without mode hop. An external cavity diode laser-ECDL (DL100) with the line width of 4 MHz is tuned to the transition of $5S_{1/2}, F=2 \leftrightarrow 5P_{1/2}, F'=2$ acting as the coupling field. The linearly polarized probe and coupling lasers are orthogonal in polarization and collinearly propagate through the atomic cell with the help of a $\lambda/2$ wave plate and a pair of polarization beam splitters (PBSs). The Helmholtz coils, applied around the atomic cell, were driven by a programmable power supply so as to produce a linear scan from 0 to 50 G of the magnetic field. The magnetic field could be either parallel or orthogonal to the laser beam propagation direction. Two positive lenses (L1 and L2) with their focus length of 15 cm are used for focusing both laser beams at the center of the atomic cell so as to improve the strength of the coupling field. The probe laser beam is completely contained in the coupling laser beam in the atomic cell so that all probed atoms have been coherently prepared, which is very important for getting the optimal EIT effect. The coupling laser (about 14.2 mW) is much stronger than the probe laser (around 1 μW) in front of the atomic cell. A photodiode is used to measure the absorbed probe laser passing through the atomic cell.

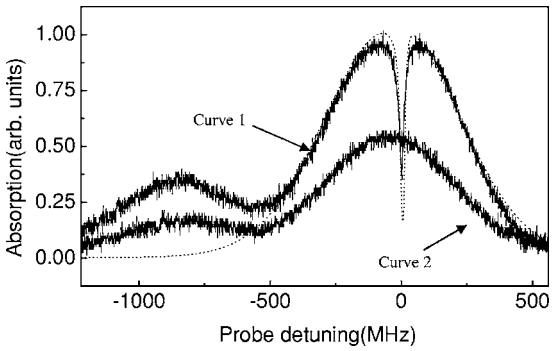

FIG. 3. Probe absorption spectra in the absence of magnetic fields. Curves 1 and 2 correspond to the experimental results with or without the coupling field, respectively. The dotted curve corresponds to the theoretical simulation with parameters of $\Omega_c = 50$ MHz, $\gamma = 6$ MHz, $\Gamma = 0.1$ MHz, $v_p = 248.0$ m/s, $\Delta_2 = 30$ MHz, and $\Delta = 30.2$ MHz.

IV. EXPERIMENTAL RESULTS AND THEORETICAL SIMULATIONS

Just by scanning the Ti:sapphire ring laser, we can get the involved absorption spectrum without EIT windows for the $D1$ transition of ^{87}Rb atoms (see curve 2 in Fig. 3). Turn on the ECDL and then adjust its current and temperature to achieve the necessary wavelength; we can observe an EIT window with contrast of about 66% in the absorption spectrum of ^{87}Rb atoms (see curve 1 in Fig. 3). Here, the parameter of contrast is defined as the ratio of the EIT depth to the height of shoulders of the EIT window. The EIT window width is about 20 MHz, which is limited by both the spontaneous decay rate of the hyperfine level $5P_{1/2}, F' = 2$ and the intensity of the Ti:sapphire ring laser. Clearly, the probe absorption (curve 1) with EIT is increased by about two times compared with that (curve 2) without EIT. The reason is that the probe field is so weak that almost all atoms are optically pumped into $5S_{1/2}, F = 1$ from $5S_{1/2}, F = 2$ via $5P_{1/2}, F' = 2$ by the coupling field (ECDL).

Turn on and then tune the programmable power supply; we can get a static magnetic field with a strength of 50 G. Keeping the magnetic field being parallel to the laser beam propagation direction, we obtain a new probe absorption spectrum as shown by Fig. 4, where the EIT window has been split into three subwindows with contrasts of about 32%, and each subwindow is about $1/\sqrt{2}$ in width as the EIT window in Fig. 3. The narrower EIT subwindows appear as the result of three sets of independent three-level systems originating from the ideal degenerate three-level system at the presence of the magnetic field. The frequency differences between any two adjacent EIT windows are 2Δ as we analyzed in Sec. II. The reduced contrast of EIT subwindows may be attributed to the mutual negative influence of different sets of independent systems. We also plot a dot curve in Fig. 4 based on Eq. (3), which demonstrates that our theoretical calculation is in good agreement with the experimental results.

In the case that the magnetic field is perpendicular to the laser beam propagation direction, we instead observe four but not three subwindows in Fig. 5 because the ideal degenerate three-level system should be divided into four sets of independent systems with different central frequencies as we analyzed in Sec. II. Contrasts of the two inner subwindows are still about 32%, while contrasts of the two outer subwindows are only about 16%. Each subwindow is about $1/\sqrt{2}$ in width like the EIT window in Fig. 3. The frequency difference between any two adjacent EIT windows is also 2Δ, which can be easily obtained by the analysis approach used in Sec. II. The subwindow widths hold independent of the split distance between adjacent subwindows because the spilt distance is only determined by the magnetic field while the subwindow widths are independent of the magnetic field. In Fig. 5, the dot curve is obtained from Eq. (4), which is also in good agreement with the experimental results. This indicates the correctness of our analysis in Sec. II again.

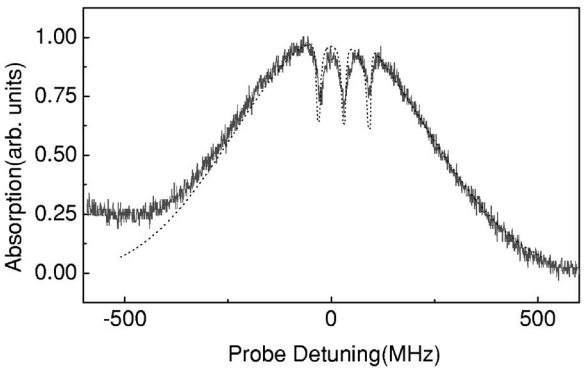

FIG. 4. Probe absorption spectra when the magnetic field is parallel to the laser propagation direction. The solid and dot curves correspond to the experimental result and the theoretical calculations, respectively. Parameters used in the theoretical simulations are $B = 43.4$ G, $\Omega_c = 50$ MHz, $\gamma = 6$ MHz, $\Gamma = 0.1$ MHz, $v_p = 248.0$ m/s, $\Delta_2 = 30$ MHz, and $\Delta = 30.2$ MHz.

Figure 6 shows the distance in frequency between any two adjacent subwindows versus the magnetic field strength when the magnetic field is perpendicular to the laser beam propagation direction. We can see that the frequency distance between adjacent subwindows linearly increases with the increase of the magnetic field strength. This is because the

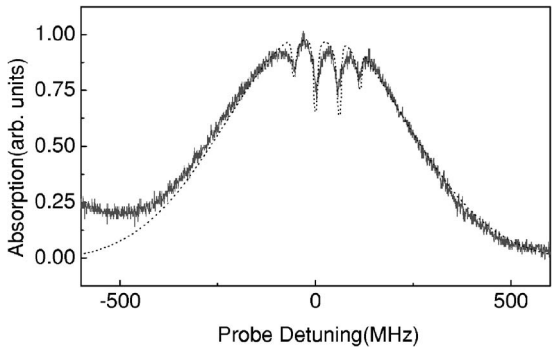

FIG. 5. Probe absorption spectra when the magnetic field is perpendicular to the laser propagation direction. The solid and dot curves correspond to the experimental result and the theoretical calculation, respectively. Parameters used in the theoretical simulations are $B = 43.4$ G, $\Omega_c = 50$ MHz, $\gamma = 6$ MHz, $\Gamma = 0.1$ MHz, $v_p = 248.0$ m/s, $\Delta_2 = 30$ MHz, and $\Delta = 30.2$ MHz.

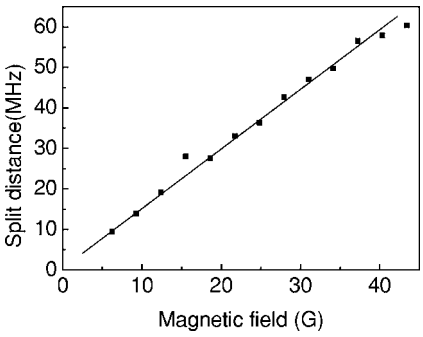

FIG. 6. Distance in frequency of adjacent EIT subwindows as a function of the magnetic field strength. Solid squares correspond to the experimental data, while the solid curve is obtained from theoretical calculation.

central frequencies of different sets of independent three-level systems are directly proportional to the strength of the magnetic field, which is clearly indicated by Eq. (1).

V. CONCLUSIONS

In summary, we have investigated both in theory and in experiment the EIT phenomenon in hot ^{87}Rb atoms with a static magnetic field being parallel or perpendicular to the laser beam direction. The experimental results show that a wide and deep EIT window can be split into three or four narrow and shallow subwindows depending on the orientation of the magnetic field. The underlying physics is that, in the limit of a weak probe field, an ideal degenerate three-level system has been split into three or four sets of independent three-level systems due to the lifting of magnetic sublevels of the involved hyperfine levels of ^{87}Rb atoms. The split independent systems have negative influence on each other, so contrasts of the split subwindows are far smaller than that of the original EIT window. Based on the density matrix equations, we also calculated the probe absorption spectra in different cases where the static magnetic field exits or not. The theoretical results are shown to be in good agreement with the experimental results. Clearly, the magnetic field could play important roles in obtaining different types of EIT effects. In order to observe the optimal EIT effect, stray magnetic fields should be avoided.

ACKNOWLEDGMENT

The authors would like to acknowledge the support from the National Natural Science Foundation under Grant No. 10334010.

[1] E. Arimondo, in *Progress in Optics*, edited by E. Wolf (Elsevier, Amsterdam, 1996), Vol. 35, p. 257.
[2] A. Imanoglu and S. E. Harris, Opt. Lett. **14**, 1344 (1989).
[3] K.-J. Boller, A. Imamoglu, and S. E. Harris, Phys. Rev. Lett. **66**, 2593 (1991); Z. X. Tang, C. M. Sorensen, K. J. Klabunde, and G. C. Hadjipanayis, *ibid.* **67**, 3602 (1991); J. Gea-Banacloche, Y. Q. Li, S. Z. Jin, and M. Xiao, Phys. Rev. A **51**, 576 (1995); Y. Q. Li, S. Z. Jin, and M. Xiao, *ibid.* **51**, R1754 (1995); Y. Q. Li and M. Xiao, *ibid.* **51**, R2703 (1995).
[4] M. O. Scully, S. Y. Zhu, and A. Gavrielides, Phys. Rev. Lett. **62**, 2813 (1989); A. S. Zibrov, M. D. Lukin, D. E. Nikonov, L. Hollberg, M. O. Scully, V. L. Velichansky, and H. G. Robinson, *ibid.* **75**, 1499 (1995); Y. Zhu, Phys. Rev. A **55**, 4568 (1997); D. Braunstein and R. Shuker, *ibid.* **68**, 013812 (2003).
[5] K. Hakuta, L. Marmet, and B. P. Stoicheff, Phys. Rev. Lett. **66**, 596 (1991); G. Z. Zhang, K. Hakuta, and B. P. Stoicheff, *ibid.* **71**, 3099 (1993); Y. Q. Li and M. Xiao, Opt. Lett. **21**, 1064 (1996).
[6] M. Xiao, Y. Q. Li, S. Z. Jin, and J. Gea-Banacloche, Phys. Rev. Lett. **74**, 666 (1995); H. Z. Zhang, X. Z. Guo, J. Y. Gao, Y. Jiang, and G. X. Jin, Z. Phys. D: At., Mol. Clusters **42**, 83 (1997); H. F. Zhang, J. H. Wu, X. M. Su, and J. Y. Gao, Phys. Rev. A **66**, 053816 (2002).
[7] J. Y. Gao *et al.*, Opt. Commun. **93**, 323 (1992); see [3].
[8] B. S. Ham and P. R. Hemmer, Phys. Rev. Lett. **84**, 4080 (2000); B. S. Ham, M. S. Shahriar, M. K. Kim, and P. R. Hemmer, Phys. Rev. B **58**, R11825 (1998).
[9] Y. C. Chen, C. W. Lin, and I. A. Yu, Phys. Rev. A **61**, 053805 (2000).
[10] A. M. Akulshin, S. Barreiro, and A. Lezama, Phys. Rev. A **57**, 2996 (1997).
[11] M. O. Scully and M. Fleischhauer, Phys. Rev. Lett. **69**, 1360 (1992); H. Lee, M. Fleischhauer, and M. O. Scully, Phys. Rev. A **58**, 2587 (1998).